4

An Inductive Self-complementary Hilbert-curve Antenna for UHF RFID Tags

Ji-Chyun Liu[1], Bing-Hao Zeng[1] and Dau-Chyrh Chang[2]
[1]*Ching Yun University Chung-Li City, Taoyuan County, Taiwan*
[2]*Oriental Institute of Technology Pan-Chiao City, Taipei County, Taiwan*
R.O.C

1. Introduction

Recently there has been a rapidly growing interest in RFID systems and its applications. Operating frequencies including 125 KHz–134 KHz and 140 KHz–148.5 KHz LF band, 13.56 MHz HF band and 868 MHz–960 MHz UHF band were applied to various supply chains. 433 MHz band was decided for active reader and 2.45 GHz band was applied for WiFi reader. Besides the reader antennas, the requirements of tag antennas are necessary for applications. In which, due to the benefit of long read range and low cost, the UHF tag will be used as the system of distribution and logistics around the world [1–13], [29–41].

Meander line antennas were commonly for UHF tags, due to the characteristics of high gain, omni-directionality, planarity and relatively small surface size [5]. However, the length-to-width ratio limited as 5:1 was proposed [2]. Recently, the half-Sierpinski fractal antenna was introduced with a small length-to-width ratio (<2:1) [11]. Meanwhile, the inductive impedance of tag antenna was necessary for matching the capacitive terminations of chip IC, thus the tuning apparatus was proposed [4], [8]–[10]. H-shaped meandered-slot antennas with the performance of broadband and conjugate impedance matching were developed for on-body applications [14], [15]. On the other hand, the self-complementary dipoles were introduced for the performance of wideband, high impedance and balun [16]–[23].

The Hilbert-curve, proposed by Hilbert and introduced by Peano [24], was known as the space-filling curves. The structure of this shape can be made of a long metallic wire compacted within a patch. As the iteration order of the curve increases, the Hilbert-curve can be space-filling the patch. It has been used in fractal antenna with size reduction [25–28], [44–52].

The main aim of this paper is to merge the meander line and meandered-slot structure of the RFID tag antenna in order to obtain a good performance of compact, broadband and conjugate impedance matching. Meantime, demonstrating the performance with a self-complementary Hilbert-curve tag antenna is proposed. The self-complementary Hilbert-curve tag antenna is constructed with substrate, Hilbert-curve, Hilbert-curve slot and tuning pad. For circular polarization analysis, the current distribution and electric field are exhibited. The inductive and broadband characteristics of frequency responses and directivity feature of radiation patterns and polarization are studied and presented.

2. Antenna configuration and basis

2.1 UFH RFID meander-line antenna

The typical dipole antenna consists of two parts, in Fig.1, one is the dipole resonators with half-wavelength for resonance and the other is the balun for the impedance transfer of balance to unbalance terminations. The standing voltage and current distribute among the dipole with maxima current and minimum voltage feeding in the center (0°) for linear polarization. For size reduction, in Fig.2, the meander-line configuration was applied in tag antenna. By tuning load-line structure, more wideband and inductive performance can be achieved.

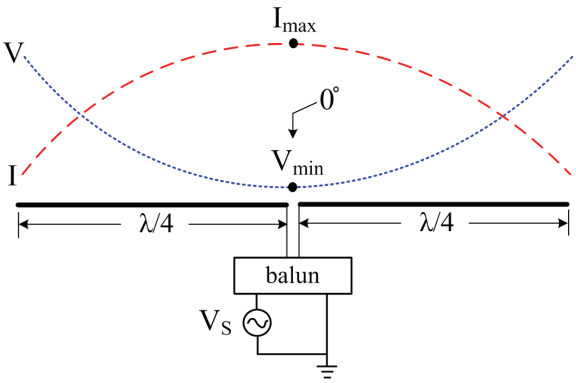

Fig. 1. Dipole antenna

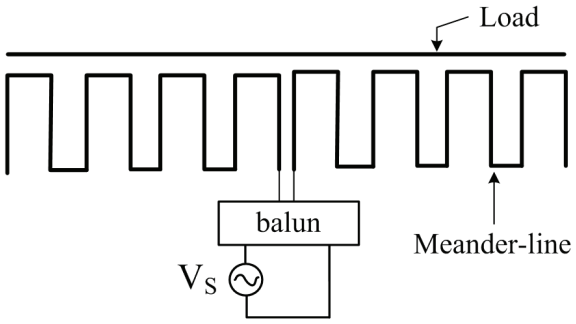

Fig. 2. Meander line antennas

2.2 Hilbert-curve and space filling

Hilbert-curve is a space filling curve with being self-similar and simple geometry. The configurations of Hilbert-curve for first four fractal iterations are shown in Figure 3. The original space has filling nature of these curves. This expresses that for a given area of a space, the total length of the line segments increase progressively as the iteration order increases. It can be interpreted as the cause for their relatively lower resonant frequency. It is evident that the fractal iteration order increases, the total length of the line segments

increases, even as the area it encompasses remain the same. Thus within a small area, a lower resonant frequency antenna with very large line length can be accommodated. In applications, the structure of this shape can be made of a long metallic wire compacted within a microstrip patch.

The topological dimension of the line segments is one, as it consists only of a line. The dimension of this original space is an integer value equated two. When we consider the length and number of line segments with 2nd, 3rd and 4th iterations, this dimension are 1.465, 1.694 and 1.834. These values point to the fact the geometry has fractional dimension. **As** the dimension approaches 2, the curve almost fills a space. In other words, for large iteration orders, the total length of the line segments tends to be extremely large. This could be a significant advantage in lower frequency antenna design since the overall effective length of the antenna is large. Thus the resonant frequency can be reduced considerably for a given area, by increasing the fractal iteration order. It may result in a larger reduction factor for the antenna size.

(a) (b) (c) (d) (e)

Fig. 3. First four fractal iterations for the Hilbert-curve configurations, (a) original space (b) 1st iterations (c) 2nd iterations (d) 3rd iterations (e) 4th iterations

2.3 Self- complementary antennas

Self-complementary antenna composed with electric and magnetic pair antennas is a potential antenna solution for multi-band and wide-band antenna system because of its excellent isolation performance at close proximity between antennas. The pair antennas can be configured with log-period, spiral and circular disk configuration depends on application shown in Fig. 4.

Antenna pair with self-complementary structure has a constant input impedance, independent of the source frequency and the antenna geometry. To achieve wideband CP performance, self-complementary structures were commonly used owing to their features of simple feeding and good axial ratio [17, 18, 23].

2.4 Self-complementary Hilbert-curve tag antenna

Complementary Hilbert-curve tag antenna is constructed with substrate, Hilbert-curve, Hilbert-curve slot and tuning pad (L_t) in Fig. 5. The Hilbert-curve is consisted of three series Hilbert-curve with the 3rd iteration. The dimensions are L_1 = 23.5 mm, L_2 = 24 mm, L_t = 5mm, W_1 = 7.5 mm, W_2 = 8.5 mm, W_3 =0.75 mm, W_4 = 0.5 mm, and g =0.35 mm. The thickness (h) of RT/duroid-6010 substrate is 6.35 mm (1.27mm×5) and the relative permittivity ε_r is 10.2 shown in Fig. 6. The length-to-width ratio is 6.2:1 and the shortening ratio SR=0.69. The reduction is notable when the SR is more than 0.40 [2].

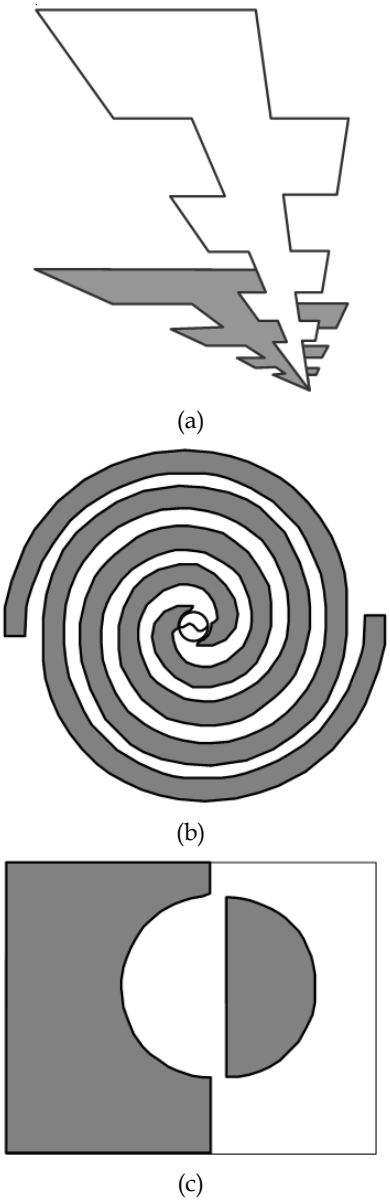

Fig. 4. Self-complementary antenna configurations, (a) log-period (b) spiral (c) circular disk

A typical circular polarization dipole cross-pair usually consist of two individuals with horizontal and vertical locations, and a two-phase signal with 90° difference. Fig. 7 illustrates the simulated current distributions and Fig. 6 depicts the simulated electric fields among the planar structures, which provide a clearly physical insight on understanding the circular polarization of the proposed antenna. Fig. 5 shows that the Hilbert-curve is excited

with concentrating current distributions at the 900 MHz resonance while the maximum amplitude located at –11.3° with deviation from central feed-line (0°). The Hilbert-curve slot is expressed with lower current distributions. Fig. 8 presents both Hilbert-curve line and Hilbert-curve slot are excited with intensive electric fields at the 900 MHz resonance while the minimum amplitude presented at –22.5°.

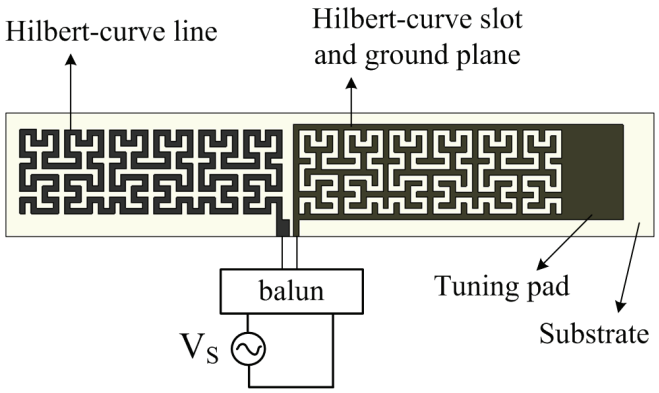

Fig. 5. Complementary Hilbert-curve antenna

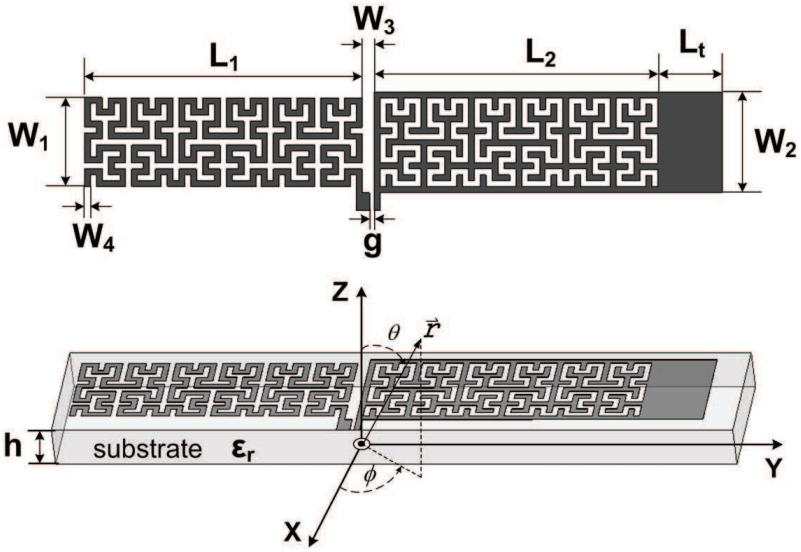

Fig. 6. Dimensions of complementary Hilbert-curve tag antenna

Since the phase difference with 33.8° among maximum current amplitude and minimum electric field existed, in company with the different locations of the left Hilbert-curve line and the right Hilbert-curve slot, the elliptic polarization will be obtained. Thus, the circular polarization can be observed along a certain direction.

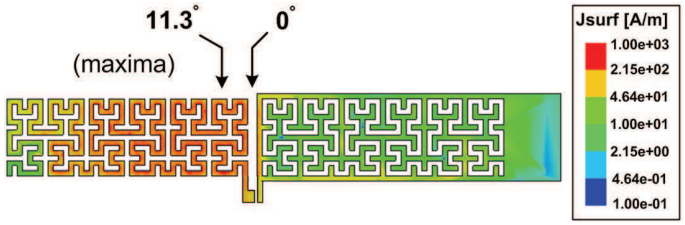

Fig. 7. Current distributions

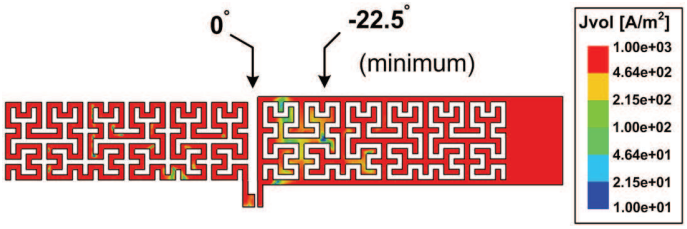

Fig. 8. Electric fields

2.5 Applications

The maximum activation distance of the tag for the given frequency is given [14]–[15] by

$$d_{\max} = \frac{c}{4\pi f}\sqrt{\frac{EIRP_R}{P_{chip}}\tau G} \tag{1}$$

Where $EIRP_R$ is the effective transmitted power of reader, P_{chip} is the sensitivity of tag microchip, G is the maximum tag antenna gain, and the power transmission factor

$$\tau = \frac{4R_{chip}R_A}{\left|X_{chip} + X_A\right|^2} \le 1 \tag{2}$$

with tag antenna impedance ($Z_A = R_A + jX_A$) and microchip impedance ($Z_{chip} = R_{chip} + jX_{chip}$).

3. Simulations and experiments

By using the commercial software of HFSS tool [42], the simulation results included return loss spectrums, impedance spectrum, circular polarization and two-cut radiation patterns are presented and analyzed. For comparison, the return loss spectrums of the proposed antenna with UHF-bands of 900 MHz are measured and simulated shown in Fig. 9.

The simulated and measured results of frequency responses are in agreement. In measurement, while the return loss is smaller than -10dB, the frequency responses cover both Europe 865.6–867.6 MHz band and USA 902–928 MHz band, ranging from 820 to 935 MHz (bandwidth = 115 MHz). For applications, the frequency responses are fully applied in the operation bands of the RFID UHF-band. For impedance spectrum analysis in Fig. 10, it shows the real parts of impedance become maximum value (178.7 Ω) at 970 MHz frequency,

the real parts of impedance value (102.5 Ω) and the imaginary parts of impedance present inductive characteristic (+41.3 Ω) at 900 MHz frequency. The inductive impedance can be available for matching the capacitive RFID chip.

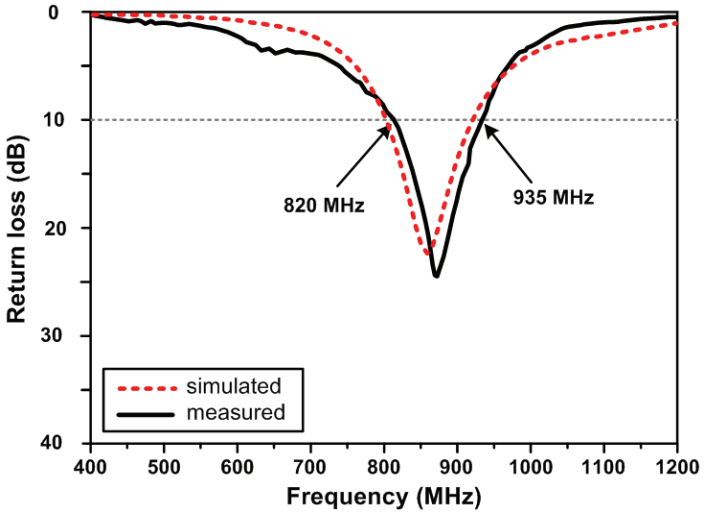

Fig. 9. Simulated and measured results of return loss spectrum

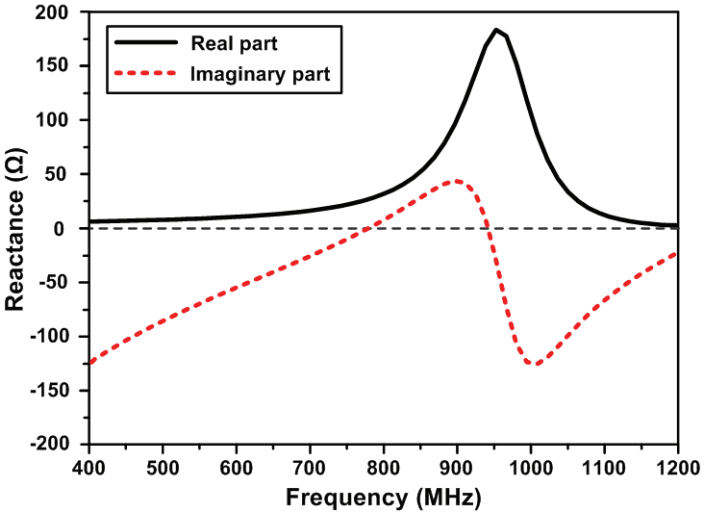

Fig. 10. Simulated results of impedance spectrum

The radiation patterns are obtained by an automatic measurement system in an anechoic chamber. The under-tested antenna is located on the X-Y plane shown in Fig. 4, and the feeding line is located along the X-axis. Thus, two radiation patterns with Y-Z cut and X-Z cut are obtained.

The two cut patterns with resonant 900 MHz are represented in Fig. 11 respectively. Broadside patterns are observed in the Y-Z cut and quasi-omnidirectional patterns are obtained in the X-Z cut. The measured maximum gain was 1.68 dBi for 900 MHz. For polarizations, the AR spectrum is presented in Fig. 12. The minimum AR with 0.16 at ϕ = 0°, θ = 90°and the right-hand circular polarizations (–3dB AR BW = 383 MHz) are observed along the direction of the ϕ and θ, thus the proposed antenna can be applied to circular polarization applications which represents one of the availabilty and usefulness in contrast to the conventional meander-line and meander-slot tags.

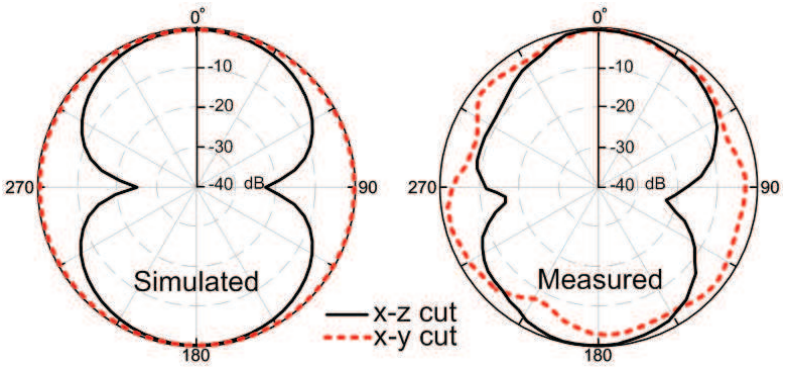

Fig. 11. Radiation patterns for 900 MHz

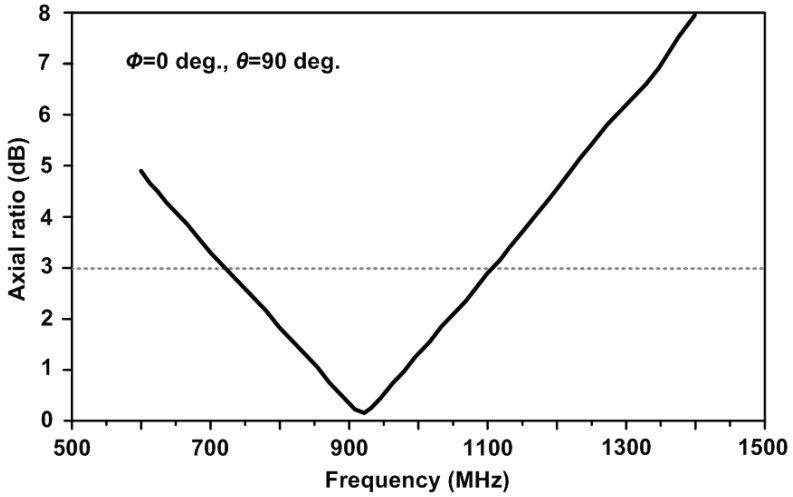

Fig. 12. AR spectrum

4. Conjugate matching performance

For example, the effective transmitted power $EIRP_R$ of reader is 1W, the sensitivity P_{chip} of tag microchip is -10dBm, the maximum tag antenna gain G = 1.62dBi, and the activation

distance $d_{min/max}$ = 2.5/3 m, the power transmission factor can be obtained τ = 0.73/0.87 by using (2). Then, from (3) and tag antenna impedance (Z_A = 102.5+j41.3 Ω), the microchip impedance (Z_{chip} = 14.7-j45.2 Ω) is calculated. For 900 MHz signal, the capacitance (757 pf) of the chip microchip is presented.

For applications, the variation in antenna impedance, microchip impedance and tuning pad (L_t = 1.0, 2.0, 3.0, 4.0 and 5.0 mm) is shown in Table I. The varied inductive impedance can be available for matching the related capacitive RFID chip (564–787 pf) by tuning the pad length.

L_t (mm)	Z_A (Ω)	G_{max} (dB)	$d_{min/max}$ (m)	$\tau_{min/max}$	Z_{chip} (Ω)
1	97.8+j46.3	0.98	2.5/3	0.71/0.96	15.6- j46.4
2	98.7+j45.6	1.12	2.5/3	0.68/0.99	14.3- j45.5
3	97.3+j44.2	1.21	2.5/3	0.78/0.98	15.7- j44.3
4	99.6+j43.4	1.38	2.5/3	0.76/0.93	14.2- j45.8
5	102.5+j41.3	1.62	2.5/3	0.73/0.87	14.7- j45.2

Table 1. Variation results

A microchip, RI-UHF-STRAP-08 of TI, is used for applications [43]. The data sheet is presented in Table 2. The diagram of complex plane $Z(\omega)$ is presented in Fig. 13. The microchip impedance locus $Z_{chip}(\omega)$ is firstly plotted in the complex plane. The arrowhead attached to the locus indicates the direction of increasing ω from 860 to 960 MHz. Then, tuning the length, as g=0.45 mm, L_f = 5.8 mm and L_t = 6.3 mm, the antenna impedance locus $Z_a(\omega)$ is obtained. The intersection of these two loci corresponds to the operating point. Due to the operating point Z_{chip} = 287+j55 Ω and Z_a = 287-j55 Ω, τ =0.54 is calculated by (2). As $EIRP_R$ =1W, P_{chip}= -13dBm and G = 1.62dBi, d_{max} =33 m is obtained by (1).

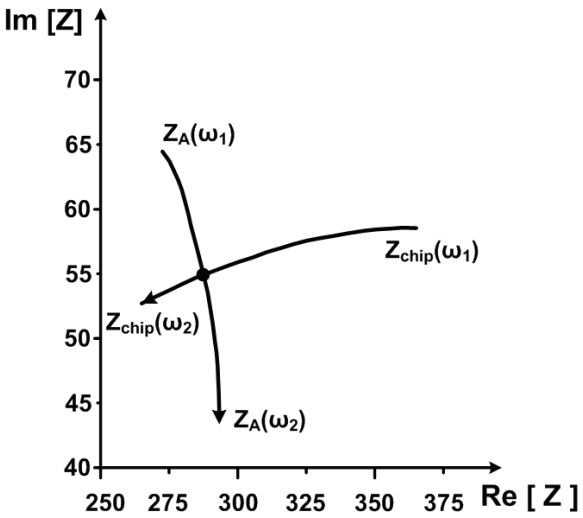

Fig. 13. Impedance locus

PART NUMBER	**RI-UHF-STRAP-08**			
Absolute Maximum Ratings				
	NOTES	**Min**	**Max**	**Unit**
Input current, pad to pad			1	mA
Input voltage to any pad (sustained)			1.5	V
Power dissipation	TA = 25°C		1.5	mW
Storage temperature range	Single Strap	-40	85	°C
	On Reel	-40	45	
Operating temperature	Read	-40	65	°C
	Write	-25	65	
Assembly survival temperature	1 minute maximum		150	°C
RF Exposure	800 ~ 1000 MHz		10	dBm
ESD immunity	Charged-Device Model (CDM)	0.5		kv
	Human-Body Model (HBM)	2		kv
Recommended Operating Conditions				
		Min	**Max**	**Unit**
T_A Operating temperature		-40	65	°C
f_{res} Carrier frequency		860	960	MHz
Electrical Characteristics				
PARAMETER	**TEST CONDITIONS**	**Min/ Max**	**Typ**	**Unit**
Sensitivity	Reading	-9/ -	-13	dBm
	Programming	-6/ -	-19	
$\Delta\Gamma$ Change in modulator reflection coefficient			>0.2	
t_{DRET} Data retention		10/ -		Years
W&E Write and erase endurance		100000/ -		Cycles
Strap Parallel Impedance	Typical Read (–13 dB)		380	Ω
			2.8	pF

Table 2. Specification of microchip RI-UHF-STRAP-08

For deterministic design, the design procedure is stated as: The guided wavelength ($\lambda_g / 2$) of the central frequency determines the total length of series Hilbert-curve. The desired response and impedance are then tuned by L_t. The final tuning is with g. Using (1) and (2) with the specifications and boundary condition $d_{1/2}$, the Z_{chip} is obtained. If it is not satisfied, retuning L_t and g till the desired value is achieved.

5. Conclusion

The self-complementary antenna with Hilbert-curve configuration for RFID UHF-band tags is presented in this paper. The good performance of compact, broadband (BW=150 MHz), circular polarization and conjugate impedance matching are achieved for applications. The

structure is smaller in size and easy to fabricate in tag circuits. Its operations cover UHF-bands 820 to 935 MHz for return loss < -10dB. Both simulation and measurement results are agreed with the verified frequency responses. The inductive impedance is achieved and be available for matching the capacitive RFID chip.
In field analysis, broadside patterns are observed in the Y-Z cut and quasi-omnidirectional patterns are obtained in the X-Z cut. The measured maximum gain was 1.68 dBi for 900 MHz. The circular polarization (–3dB AR BW = 383 MHz) feature of radiation patterns for 900 MHz are presented. It is a compact and available tag antenna for UHF RFID applications.

6. References

[1] Marrocco, G. (2003). Gain-optimized self-resonant meander line antennas for RFID applications. *IEEE Antennas Wireless Propag. Lett.*, Vol. 2, pp. 302–305, ISSN: 1536-1225.

[2] Keskilammi, M. & Kivikoski, M. (2004). Using text as a meander line for RFID transponder antennas. *IEEE Antennas Wireless Propag. Lett.*, Vol. 3, pp. 372–374, ISSN: 1536-1225.

[3] Ukkonen, L.; Sydanheimo, L. & Kivikoski, M. (2005) Effects of metallic plate size on the performance of microstrip patch-type tag antennas for passive RFID. *IEEE Antennas Wireless Propag. Lett.*, Vol. 4, pp. 410–413, ISSN: 1536-1225.

[4] Son, H.W. & Pyo, C.S. (2005). Design of RFID tag antennas using an inductively coupled feed," *Electron. Lett.*, Vol. 41, No. 18, pp. 994–996, ISSN: 0013-5194.

[5] Rao, K.V.S.; Nikitin, P.V. & Lam, S.F. (2005). Antenna design for UHF RFID tags: a review and a practical application. *IEEE Trans. Antennas Propag.*, Vol. 53, No. 12, pp. 3870–3876, ISSN: 0018-926X.

[6] Ukkonen, L.; Schaffrath, M.; Engels, D.W.; Sydanheimo, L. & Kivikoski, M. (2006). Operability of folded microstrip patch-type tag antenna in the UHF RFID bands within 865-928 MHz. *IEEE Antennas Wireless Propag. Lett.*, vol. 5, pp. 414–417, ISSN: 1536-1225.

[7] Chang, C.C. & Lo, Y.C. (2006). Broadband RFID tag antenna with capacitively coupled structure," *Electron. Lett.*, Vol. 42, No. 23, pp. 1322–1323, ISSN: 0013-5194.

[8] Son, H.W.; Choi, G.Y. & Pyo, C.S. (2006). Design of wideband RFID tag antenna for metallic surfaces. *Electron. Lett.*, Vol. 42, No. 5, pp. 263–265, ISSN: 0013-5194.

[9] Ahn, J.; Jang, H.; Moon, H. Lee, J.W. & Lee, B. (2007). Inductively coupled compact RFID tag antenna at 910 MHz with near-isotopic radar cross-section (RCS) patterns. *IEEE Antennas Wireless Propag. Lett.*, Vol. 6, pp. 518–520, ISSN: 1536-1225.

[10] Hu, S.; Law, C.L. & Dou, W. (2007). Petaloid antenna for passive UWB-RFID tags. *Electron. Lett.*, Vol. 43, No. 22, pp. 1174–1176, ISSN: 0013-5194.

[11] Vemagiri, J.; Balachandran, M.; Agarwal, M. & Varahramyan, K. (2007). Development of compact half-sierpinski fractal antenna for RFID applications. *Electron. Lett.*, Vol. 43, No. 22, pp. 1168–1169, ISSN: 0013-5194.

[12] Kim, K.H.; Song, J.G.; Kim, D.H.; Hu, H.S. & Park, J.H. (2007). Fork-shaped RFID tag antenna mountable on metallic surfaces. *Electron. Lett.*, Vol. 43, No. 23, pp. 1400–1402, ISSN: 0013-5194.

[13] Olsson, T.; Hjelm, M.; Siden, J. & Nilsson, H.E. (2007). Comparative robustness study of planar antenna. *IET Microw. Antennas Propag.*, Vol. 1, No. 3, pp. 674–680, ISSN: 1751-8725.

[14] Marrocco, G. (2007). RFID antennas for the UHF remote monitoring of human subjects. *IEEE Trans. Antennas Propag.*, Vol. 55, No. 6, pp. 1862–1870, ISSN: 0018-926X.

[15] Calabrese, C. & Marrocco, G. (2008). Meandered-slot antennas for sensor-RFID tags. *IEEE Antennas Wireless Propag. Lett.,* Vol.7, pp. 5–8, ISSN: 1536-1225.

[16] Mushiake, Y. (1992). Self-complementary antennas. *IEEE Antennas Propag. Mag.,* Vol. 34, No. 6, pp. 23–29, ISSN: 1045-9243.

[17] Mushiake Y. (2004). A report on Japanese developments of antennas from yagi-uda antenna to self-complementary antennas,"*IEEE Antennas Propag. Mag.*, Vol. 46, No. 4, pp. 47–60, ISSN: 1045-9243.

[18] Xu, P.; Fujimoto, K. & Lin, S. (2002). Performance of quasi-self-complementary antenna Using a monopole and a slot, *Proceeding of IEEE Int. Symp. Antennas and Propag.*, pp. 464–477, ISBN: 0-7803-7330-8, San Antonio, Texas, June 2002, USA.

[19] Xu, P. & Fujimoto, K. (2003). L-shape self-complementary antenna, *Proceeding of IEEE Int. Symp. Antennas and Propag.*, pp. 95–98, ISBN: 0-7803-7846-6, Columbus, Ohio, June 2003, USA.

[20] Mosallaei, H. & Sarabandi, K. (2004). A Compact Ultra-wideband Self-complementary Antennas with Optimal Topology and Substrate, *Proceeding of IEEE Int. Symp. Antennas and Propag.*, pp. 1859–1862, ISBN: 0-7803-8302-8, Monterey, California June 2004, USA.

[21] Saitou, A.; Iwaki, T.; Honjo, K.; Sato, K.; Koyama, T. & Watnabe, K. (2004). Practical realization of self-complementary broadband antenna on low-loss resin substrate for UWB applications, *Proceeding of Int. IEEE MTT-S, Microw. Symp. Digest,* pp. 1265–1268, ISBN: 0-7803-8331-1, YKC Corp., October 2004, Tokyo, Japan.

[22] Wong, K.L.; Wu, T.Y.; Su, S.W. & Lai, J.W. (2003). Broadband printed quasi-self-complementary antenna for 5.2/5.8 GHz operation. *Microwave Opt. Technol. Lett.*, Vol. 39. No. 6, pp. 495-496, ISSN: 1098-2760.

[23] Chen, W.S.; Chang, C.T. & Ku, K.Y. (2007). Printed triangular quasi-self-complementary antennas for broadband operation, *Proceeding of Int. Symp. Antennas and Propag.*, pp. 262–265, Niigata University, August 2007, Niigata, Japan.

[24] Sagan, H. (1994). Space-filling curves, Springer-Verlag, ISBN: 3-540-94265-3, New York.

[25] Anguera, J.; Puente, C. & Soler, J. (2002). Miniature monopole antenna based on the fractal Hilbert curve, *Proceeding of IEEE Int. Symp. Antennas and Propag.*, Vol. 4, pp. 546–549, ISBN: 0-7803-7330-8, San Antonio, Texas, June 2002, USA.

[26] Best, S.R. & Morrow, J.D. (2002). The effectiveness of space-filling fractal geometry in lowering resonant frequency. *IEEE Antennas Wireless Propag. Lett.*, Vol. 1, pp. 112–115, ISSN: 1536-1225.

[27] Gonzalez-Arbesu, J.M.; Blanck, S. & Romeu, J. (2003). The Hilbert curve as a small self-resonant monopole from a practical point of view. *Microwave Opt. Technol. Lett.*, Vol.39, No. 1, pp. 45–49, ISSN: 1098-2760.

[28] Yang, X.S.; Wang, B.Z. & Zhang, Y. (2006). Two-port reconfigurable Hilbert curve patch antenna. *Microwave Opt. Technol. Lett.*, Vol. 48, No. 1, pp. 91–93, Jan. 2006. ISSN: 1098-2760.

[29] Rathod, J.M. & Kosta, Y.P. (2009). Low cost development of RFID antenna, *Proceeding of Asia Pacific. Microwave Conference,* Vol. 7, NO. 10, pp. 1060-1063, ISBN: 978-1-4244-2801-4. Dec. 2009, Singapore.

[30] Toccafondi, A. & Braconi, P. (2007). Compact meander line antenna for HF-UHF tag integration. *Proceeding of IEEE Int. Symp. Antennas and Propag.*, Vol. 9, NO. 15, pp. 5483-5486 , ISBN: 978-1-4244-0877-1, June 2007, Hawaii.

[31] Kin, S.L.; Mun, L.N. & Cole, P.H. (2007). Miniaturization of Dual Frequency RFID Antenna with High Frequency Ratio. *Proceeding of IEEE Int. Symp. Antennas and Propag.*, Vol. 9, No. 15, pp. 5475-5478 , ISBN: 978-1-4244-0877-1, June 2007, Hawaii.

[32] Roudet, F.; Vuong, T.P. & Tedjini, S. (2007). Metal effects over 13.56 MHz RFID reader antenna in an electrical switchboard. *Proceeding of IEEE Int. Symp. Antennas and Propag.*, Vol. 9, NO. 15, pp. 2777-2780, ISBN: 978-1-4244-0877-1. June 2007, Hawaii.

[33] Pengcheng, L.; Yu, J.R. & Chieh, P.L. (2008). A experiment study of RFID antennas for RF detection in liquid solutions. *Proceeding of IEEE Int. Symp. Antennas and Propag.*, Vol. 5, NO. 11, pp. 1-4, ISBN: 978-1-4244-2041-4. July 2008, San Diego, CA.

[34] Toccafondi, A.; Giovampaola. C.D.; Mariottini, F. & Cucini, A. (2009). UHF-HF RFID integrated tag for moving vehicle identification. *Proceeding of IEEE Int. Symp. Antennas and Propag.*, Vol. 1, NO. 5, pp. 1-4, ISBN: 978-1-4244-3647-7. June 2009, Charleston, SC.

[35] Iliev, P.; Le Thuc, P.; Luxey, C. & Staraj, R. (2009). Dual-band HF-UHF RFID tag antenna. *Electron. Lett.,* Vol. 45, NO. 9, pp. 439-441, ISBN: 0013-5194.

[36] Hirvonen, M.; Pesonen, N.; Vermesan, O.; Rusu, C. & Enoksson, P. (2008). Multi-system, multi-band RFID antenna: Bridging the gap between HF- and UHF-based RFID applications. *Proceeding of European Microwave Conference on Wireless Technol.,* Vol. 27, No. 28, pp. 346-349, ISBN: 978-2-87487-008-8. Oct. 2008, Amsterdam.

[37] Wang, D.; Xu, L.; Huang, H. & Sun, D. (2009). Optimization of Tag Antenna for RFID System. *Proceeding of Information Technology and Computer Science on International Conference,* Vol. 2, No. 26, pp. 36-39, ISBN: 978-0-7695-3688-0. July 2009, Kiev.

[38] Bassen, H.; Seidman, S.; Rogul, J.; Desta, A. & Wolfgang, S. (2007). An Exposure System for Evaluating Possible Effects of RFID on Various Formulations of Drug Products. *Proceeding of IEEE Int. Conference on RFID,* Vol. 26, NO 28, pp. 191-198, ISBN: 1-4244-1013-4. March 2007, Grapevine, TX.

[39] Allen, M.L.; Jaakkola, K.; Nummila, K. & Seppa, H. (2009). Applicability of Metallic Nanoparticle Inks in RFID Applications. *IEEE Trans. Components and Packaging Technologies,* Vol. 32, No. 2, pp. 325-332, ISBN: 1521-3331.

[40] Mayer, L.W. & Scholtz, A.L. (2008). A Dual-Band HF / UHF Antenna for RFID Tags. *Proceeding of IEEE 68th Vehicular Technology Conference,* Vol. 21, No. 24, pp. 1-5, ISBN: 1090-3038. Sept. 2008, Calgary, BC.

[41] Kariyapperuma, A.V. & Dayawansa, I.J. (2009). Bi-loop' RFID reader antenna for tracking fast moving tags. *Proceeding of IEEE Radio and Wireless Symposium,* Vol. 18, No. 22, pp. 449-452, ISBN: 978-1-4244-2698-0. Jan. 2009, San Diego, CA. HFSS version 11.0, Ansoft Software Inc., 2007. Texas Instruments Incorporated, http://www.ti.com/.

[42] Vinoy, K.J.; Jose, K.A.; Varadan, V.K. & Varadan, V.V. (2001). Resonant Frequency of Hilbert Curve Fractal Antennas. *Proceeding of IEEE Int. Symp. Antennas and Propag.*, Vol. 3, pp. 648–4651, ISBN: 0-7803-7070-8. July 2001Boston, MA.

[43] Vinoy, K.J.; Jose, K.A.; Varadan, V.K. & Varadan, V.V. (2001) Hilbert Curve Fractal Antennas with Reconfigurable Characteristics. *Inte. Microwave Symposium Digest, IEEE MTT-S l.* Vol.1, pp.381-384, ISBN: 0-7803-6538-0. 2001, Phoenix, AZ.

[44] Yang, X.S.; Wang, B.Z. & Zhang, Y. (2005). A Reconfigurable Hilbert Curve Patch Antenna. *Proceeding of IEEE Int. Symp. Antennas and Propag*., Vol.2B, pp.613-616, ISBN: 0-7803-8883-6. July 2005.

[45] Murad, N.A.; Esa, M.; Yusoff, M.F.M.; & Ali, S.H.A. (2006). Hilbert Curve Fractal Antenna for RFID Application. *Inte. RF and Microwave Conference,* pp.182-186, ISBN: 0-7803-9745-2. Sept. 2006, Putra Jaya.

[46] Takemura, N. (2009). Inverted-FL antenna with self-complementary structure. *IEEE Trans. Antennas Propag*., Vol. 57, No.10 , pp. 3029–3034, ISSN : 0018-926X.

[47] Suh, S.Y.; Nair, V.K.; Souza, D. & Gupta, S. (2007). High isolation antenna for multi-radio antenna system using a complementary antenna pair. *Proceeding of IEEE Int. Symp. Antennas and Propag.*, pp.1229-1232, ISBN: 978-1-4244-0877-1. June 2007, Honolulu, HI.

[48] Guo, L.; Chen, X. & Parini, C.G. (2008). A Printed Quasi-Self-Complementary Antenna for UWB Applications. *Proceeding of IEEE Int. Symp. Antennas and Propag.,* pp.1-4, ISBN: 978-1-4244-2041-4. July 2008, San Diego, CA.

[49] Guo, L.; Wang, S.; Chen, X. & Parini, C. (2009). A Small Printed Quasi-Self-Complementary Antenna for Ultrawideband Systems. *IEEE Antennas Wireless Propag*. Vol.8, 2009, pp.554-557, ISSN : 1536-1225.

[50] Xu, P.; Kyohei F. & Shiming L. (2002). Performance of Quasi-Selfcomplementary Antenna Using a Monopole and a Slot. *Proceeding of IEEE Int. Symp. Antennas and Propag.,* pp.464-467, ISBN: 0-7803-7330-8. 2002.

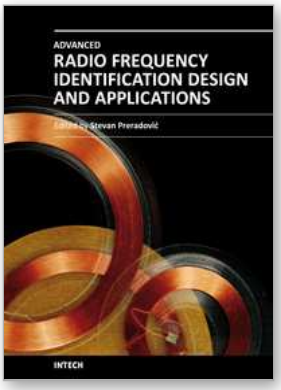

Advanced Radio Frequency Identification Design and Applications

Edited by Dr Stevan Preradovic

ISBN 978-953-307-168-8
Hard cover, 282 pages
Publisher InTech
Published online 22, March, 2011
Published in print edition March, 2011

Radio Frequency Identification (RFID) is a modern wireless data transmission and reception technique for applications including automatic identification, asset tracking and security surveillance. This book focuses on the advances in RFID tag antenna and ASIC design, novel chipless RFID tag design, security protocol enhancements along with some novel applications of RFID.

How to reference

In order to correctly reference this scholarly work, feel free to copy and paste the following:

Ji-Chyun Liu, Bing-Hao Zeng and Dau-Chyrh Chang (2011). An Inductive Self-complementary Hilbert-curve Antenna for UHF RFID Tags, Advanced Radio Frequency Identification Design and Applications, Dr Stevan Preradovic (Ed.), ISBN: 978-953-307-168-8, InTech, Available from: http://www.intechopen.com/books/advanced-radio-frequency-identification-design-and-applications/an-inductive-self-complementary-hilbert-curve-antenna-for-uhf-rfid-tags

INTECH
open science | open minds

InTech Europe
University Campus STeP Ri
Slavka Krautzeka 83/A
51000 Rijeka, Croatia
Phone: +385 (51) 770 447
Fax: +385 (51) 686 166
www.intechopen.com

InTech China
Unit 405, Office Block, Hotel Equatorial Shanghai
No.65, Yan An Road (West), Shanghai, 200040, China
中国上海市延安西路65号上海国际贵都大饭店办公楼405单元
Phone: +86-21-62489820
Fax: +86-21-62489821